Mechanism and kinetic studies of the adsorption of congo red on three adsorbent materials

ABSTRACT

The enormous loss of agroforestry resources should attract the attention of the scientific community. A cultivated plant has more unused organs than those harvested by the grower. For an agroforestry resource to be put to good use, its parts, previously considered waste, must be exploited for profit. This is why this study examined the potential of the hulls of *Lophira lanceolata*, an agricultural waste product, as a precursor for adsorbent materials such as activated carbon and composite materials. The two adsorbent materials are obtained by impregnation with orthophosphoric acid in a 2:1 ratio, followed by activation and pyrolysis at 500°C. The use of these adsorbent materials and clay for the removal of Congo red has proved effective, with removal rates more than 90 %. Adsorption on these materials is chemical in nature and occurs on energetically heterogeneous surfaces, which fits well with the pseudo-second-order kinetic model and Freundlich isotherms. The estimated q_{max} values for the Langmuir model are 145.0, 362, and 452 $mg.g^{-1}$ for clay, composite material and activated carbon respectively. The hulls of *Lophira lanceolata* could be used to obtain various adsorbent materials for eliminating anionic dyes from industrial wastewater in order to comply with discharge standards.

Keywords: *Biomass, clay, Lophira lanceolata, anionic dye, adsorption*

1. INTRODUCTION

Human health and the ecosystem are threatened by rapid industrialization, urbanization and population growth that have accelerated the contamination of water resources by organic pollutants[1,2].Effluents from dye manufacturing and use units and similar industries often contain large amounts of dyes and suspended organic compounds [3]. The elimination of synthetic dyes in nature has become very important, because some dyes and their derivatives are carcinogenic and toxic, therefore, it cannot depend on biodegradation alone.

“Anionic dyes (direct, acidic, and reactive dyes), cationic dyes (basic dyes), and non-ionic dyes (dispersive dyes) are the three main categories of chemical dyes”[4]. “Methylene blue is a cationic dye often used as a reference molecule in laboratory adsorption tests. It is used in textiles, cosmetics, paper coatings and medical applications. Exposure to methylene blue causes increased heart rate, vomiting, cyanosis, hypertension and tissue necrosis in humans if ingested or in contact with the skin, etc”[4,5]The researchers showed that methylene blue is effectively processed by adsorption on different adsorbent materials[6–8].

In view of this work, adsorption is widely used, which confirms its great capacity for the removal of dyes from water. In addition, it is noted that sludge-free treatments are gaining more and more importance over conventional methods, such as coagulation and flocculation.

Adsorption is a physicochemical phenomenon that takes place on the surface of solid materials called adsorbents. Among these materials, we have activated carbons, mineral adsorbents (clay, zeolite, activated alumina and silica gel) and synthetic adsorbents made from polymers. The efficiency of the adsorbents is due to physicochemical and textural properties such as porosity, specific surface, surface functions, density, etc. Apart from the cost, these properties lead to further research to find more efficient adsorbents more adapted to the molecules to be treated.

A comparative study of the adsorption of Congo red from three adsorbents, such as white clay, activated carbon, and the composite material developed from white clay and Lophira lanceolata hulls, was performed. The adsorption capacity, isotherm and adsorption kinetics were analysed and discussed.

2. MATERIALS AND METHODS

2.1. Materials

The plant material consisted of *Lophira lanceolata* hulls collected in Toucountouna, a commune located in northwestern Benin. The white clay used was collected in Sè, a locality in the commune of Houéyogbé in the Mono department located in southwestern Benin (Fig. 1). NaOH (Merck) was used to remove mineral matter from the biomass. H_3PO_4 (Merck) was used as an activating agent.

Hydrochloric acid (Merck) to wash the activated carbons. Congo red (Merck) are used as adsorbates to test the performance of the three adsorbent materials produced.

Fig.1.The map locating the place of collection of the clay

2.2. Production of adsorbent materials

The natural clay used in this study is non-pretreated. It was ground, sieved to 100nm and then dried at 105°C for at least 24 hours and then stored in a dry place.

The collected *Lophira lanceolata* hulls were grinded and sieved manually on a 2 mm mesh sieve. The shreds were washed with tap water and deionized with distilled water. It was dried at 105°C for at least 24 hours and then stored in a dry place. Then, the crushed*Lophira lanceolata* shell was washed with a molar solution of soda and dried in an oven at 105°C for at least 24 hours. The pretreated biomass was impregnated with orthophosphoric acid at impregnation ratio 2. Carbonization was done in a high temperature oven at 500°C for 2h following the gradient of 10°C/min. The pyrolysate was cooled inside the oven before being removed. A composite material was produced under the same conditions as the activated carbon by substituting part of the biomass with clay at the ratio ($m_{Biomass} : m_{clay}$):4:1.

The activated carbon obtained, and the composite material are coded as CA - CLL_2 and MC_2 respectively and then the biomass is the hull of *Lophira lanceolata.*

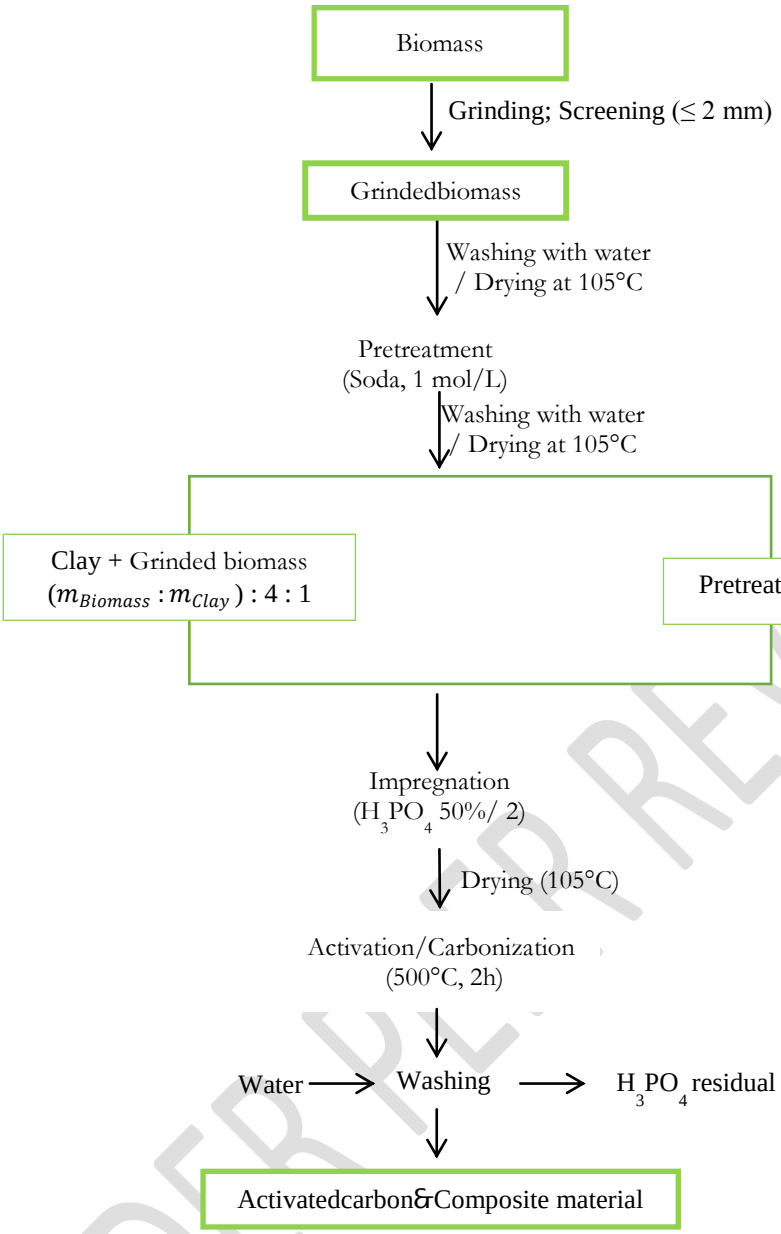

Fig. 2. Different steps in the elaboration the adsorbants

2.3. Study of the adsorption of chemical dyes on adsorbent materials

2.3.1. Effect of contact time and initial concentration

Adsorption was studied as a function of time to determine the amount of dye adsorbed at different time intervals and the equilibrium time. A mass m of activated carbon was suspended in a solution of volume V and initial concentration C_0. Samples were taken at predetermined time intervals and separated using a syringe equipped with filters (0,45µm). The analysis of the residual concentration of the adsorbats (Table1) was performed by UV-Visible absorption spectrophotometry, where the dye solution absorbs more light. The results obtained are plotted in the form of curves $q_t = f(t)$ and $R(\%) = f(t)$. The amount of adsorbed dye $q_t\ (mg/g)$ and the removal rate R (%) are calculated as follows[9–11]:

$$\mathbf{q_t} = \frac{(\mathbf{C_0} - \mathbf{C}) \times \mathbf{V}}{\mathbf{m}} \quad (1)$$

$$\mathbf{R}(\%) = \frac{\mathbf{C_0} - \mathbf{C}}{\mathbf{C_0}} \times \mathbf{100} \quad (2)$$

where C_0 and C are the initial and at time t (min) of adsorbates concentration ($mg.L^{-1}$), V the volume of solution (L) and m the dry weight of the added adsorbent (g).

Table 1. Informations on the molecule that were the subject of this study

Usual name	Red Congo
Gross formula	$C_{32}H_{22}N_6O_6S_2Na_2$
Semi-developed formula[12]	
IUPAC name	Acide benzidinediazo-bis-1-naphtylamine-4-sulfonique
Wavelength (nm)	500
Molecular molar mass ($g.mol^{-1}$)	696.66

2.3.2. Kinetic study of the adsorption of chemical dyes on adsorbent materials[13–15]

The study of adsorption kinetics is important to be able to define the adsorption efficiency. To study the kinetics and determine its parameters, the experimental data were analyzed using pseudo-first order, pseudo-second order, Elovich and intraparticle diffusion models.

2.3.3. Modelling adsorption isotherms

The Langmuir, Freundlich and Tempkin approaches are the most widely used for modelling experimental data from adsorption tests [13–15].

2.3.4. Error functions used in the selection of appropriate models

The coefficient of determination (R^2), the sum of square errors (SSE, %) and the average relative error (ARE, %) are used by comparing the experimental data and the results predicted by each model.The higher the R^2 value, the average relative error and sum of square errors, the better the fit. The sum or error squares (SSE, %) given by[16]:

$$\boldsymbol{SSE}\ (\%) = \frac{\sum_{i=1}^{N}(q_{e,exp}-q_{e,cal})_i^2}{N} \quad (3)$$

The average relative error (ARE, %) given by[16]Lütke and al., 2019):

$$\boldsymbol{ARE}(\%) = \frac{100}{N}\sum_{i=1}^{N}\left|\frac{q_{e,exp}-q_{e,cal}}{q_{e,exp}}\right|_i \quad (4)$$

where N is the number of data points.

3. RESULTS & DISCUSSION

3.1. Influence of contact time and initial concentration on the adsorption capacity of Congo red

Figs.3 show that the amount and rate of adsorption of Congo red increases rapidly during the first 5 minutes of contact and saturation is reached after 10 minutes of reaction. Figs.3 show that the composite material has the highest adsorbed amounts of Congo red and the clay the lowest. In addition, Fig.4 shows that the adsorbed amount of Congo red increases with the initial concentration.

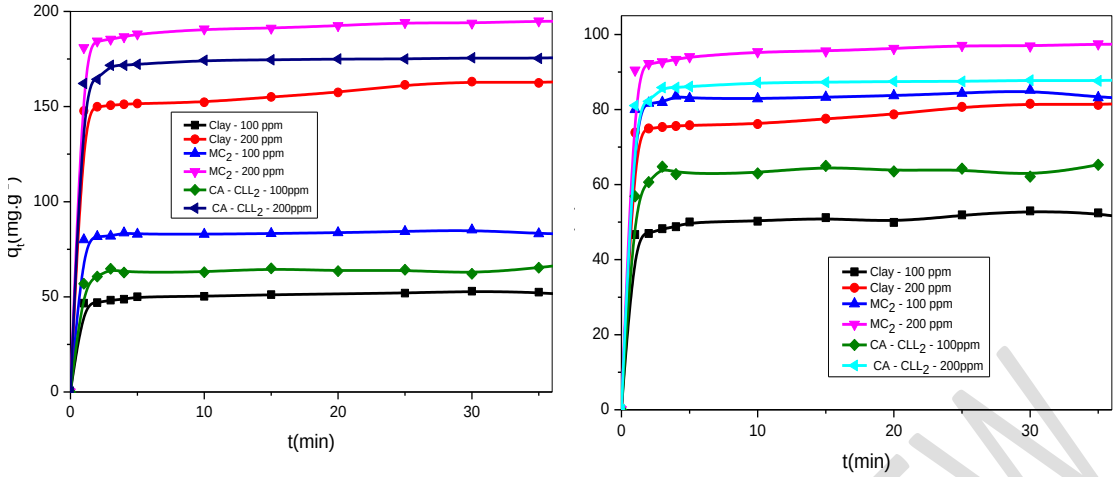

Fig. 3.Influence of time and initial concentration on the amount and rate of adsorption of Congo red by three adsorbents

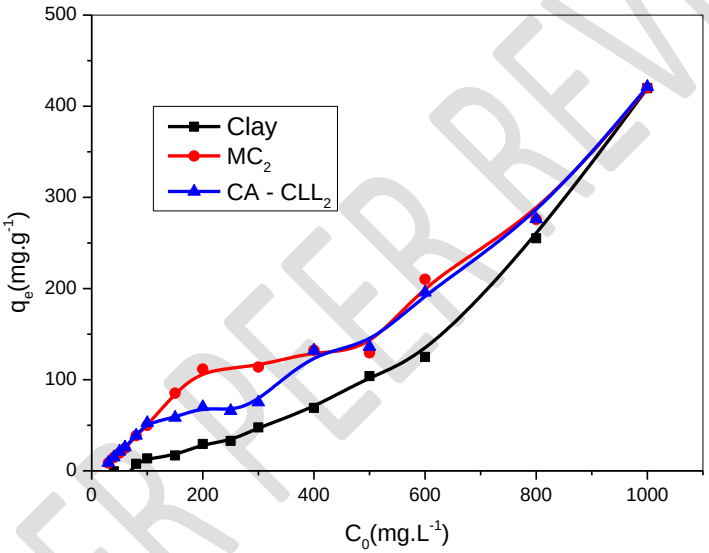

Fig.4.Effect of initial concentration on the adsorption capacity of red Congo on the three adsorbents.

3.2. Adsorption kinetics of red Congo on the adsorbent materials

This study allows us to describe the rates of the phenomenon as a function of reaction time by four kinetic laws that are represented in Figs.5, 6, 7 and 8. These kinetic models were applied to the adsorption of Congo red on the three materials. The coefficients of determination of the pseudo-second order kinetic model are the highest (Table 2), so it is the most appropriate to explain this adsorption process. In addition, this model has the closest calculated adsorbed quantities to the experimentally obtained quantities; its SES (%) and ARE (%) are the lowest (Table 2). This indicates that the adsorption of Congo wheel molecules is perfectly consistent with the pseudo-second order reaction and that the adsorption process of these molecules is controlled by chemisorption. The intraparticle diffusion model plotted must be linear if intraparticle diffusion is involved in the adsorption process and when these curves pass through the origin of the benchmark, such is not. Therefore, this indicates some degree of boundary layer control and shows that intraparticle diffusion is not the only rate-limiting step, but that other kinetic models can control the adsorption rate, all of which can operate simultaneously. Figs.7 shows that the curves are multilinear over the entire selected time range, implying that more than one process affects the adsorption, and that the adsorption process contains both surface adsorption and diffusion within the solid support.

♦ **kinetics pseudo-first-order of Cono red adsorption**

Fig.5 presented the linearized forms of pseudo-first order kinetic.

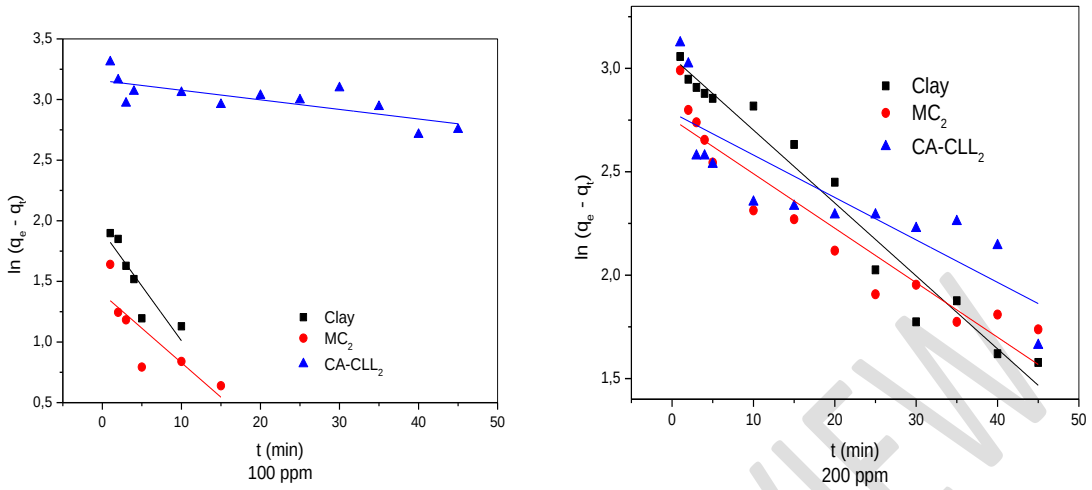

Fig.5. Linearized forms of the pseudo-first-order model for the adsorption of Congo red on adsorbent materials.

♦ **Kinetics pseudo-second order**

Fig.6. presented the linearized forms of pseudo-second order kinetic.

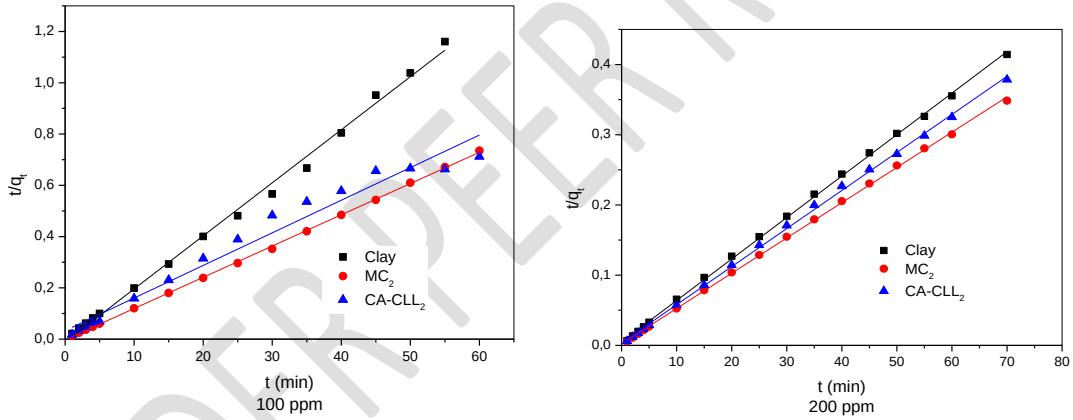

Fig.6.Linearized forms of the pseudo-second-order model for the adsorption of Congo red on adsorbent materials

♦ **Intraparticle diffusion**

Figs.7 presented the intraparticle diffusion of Congo red molecules.

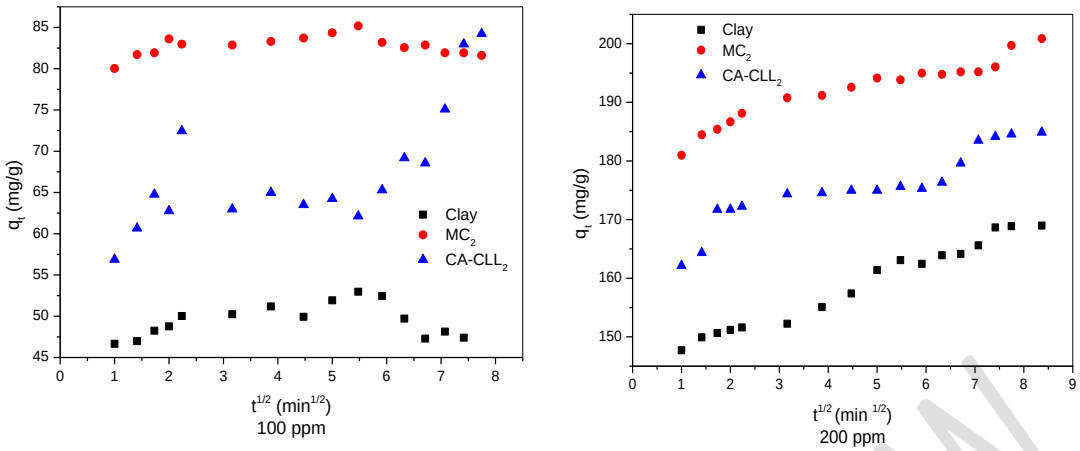

Fig.7. Intraparticle diffusion for the adsorption of Congo red on adsorbent materials.

♦ **Modèle cinétique d'Elovich**

Figs.8 present the linearized forms of the Elovich model of the adsorption of Congo red molecules.

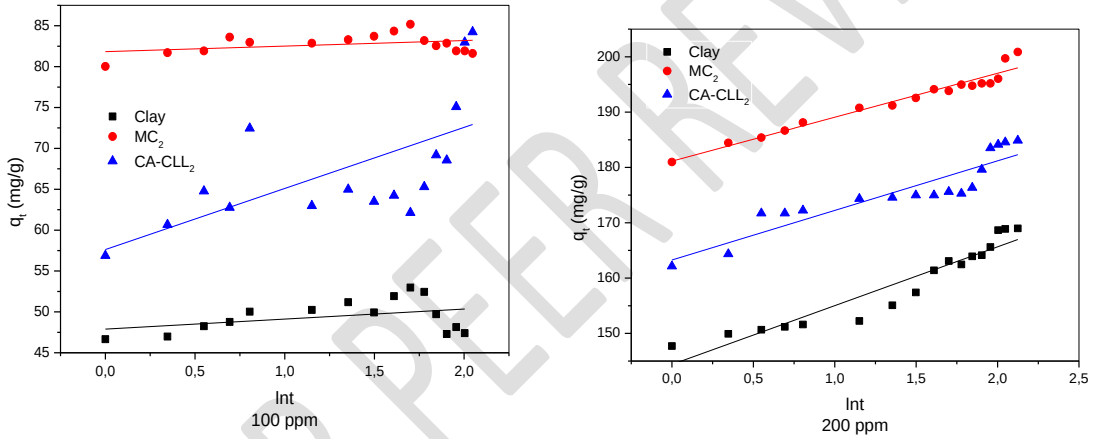

Fig. 8. Linearized forms of the Elovich model for the adsorption of Congo red on adsorbent materials

Table2. Kinetic parameters of Congo red adsorption.

		Clay		MC_2		$CA\text{-}CLL_2$	
	C_0 (mg/L)	100	200	100	200	100	200
	$q_{e,exp}$(mg/g)	53.0	169.0	85.0	200	84.0	185.0
	$q_{e,cal}$(mg/g)	6.77	21.20	4.05	15.70	23.47	16.22
Pseudo-first order	K_1 (min^{-1})	0.09	0.04	0.06	0.03	0.008	0.02
	r_1^2	0.7453	0.9628	0.5461	0.8932	0.4445	0.7037
	SSE (%)	356.0	1680.0	1097.0	2637.0	308.0	2188.0
	ARE (%)	14.54	6.72	15.87	7.09	6.01	7.02
	$q_{e,cal}$ (mg/g)	48.31	169.5	82.0	200	78.7	0.02
Pseudo-second ordre	K_2(min^{-1})	0.04	0.007	0.06	0.01	0.005	0.008
	r_2^2	0.9960	0.9994	0.9997	0.9996	0.9719	0.9990
	SSE (%)	1.44	0.015	0.62	0.04	1.98	0.01
	ARE (%)	0.58	0.02	0.23	0.03	0.42	0.01
Elovich model	α	$1.50.10^6$	$2.57.10^7$	$4.76.10^{15}$	$6.27.10^{10}$	$1.67.10^4$	$7.33.10^8$
	β	0.28	0.10	0.44	0.13	0.133	0.11

	R^2	0.9651	0.9078	0.8221	0.954	0.4087	0.8441
Intraparticle diffusion	k_i	1.20	3.02	80.56	2.15	2.36	2.46
	C	46.14	145.0	0.69	182.0	57.01	24.76
	R^2	0.9177	0.9786	0.7191	0.9322	0.5038	0.4609

3.3. Adsorption isotherms of Congo red on adsorbent materials

The isotherms of the adsorption of Congo red on the three adsorbent materials show the beginning of an S-type isotherm even if the equilibrium is not reached (Fig.9). An adsorption in which the interactions between the molecules but also with the adsorbent intervene. Consequently, the adsorption of Congo red is multilayer and cooperative.

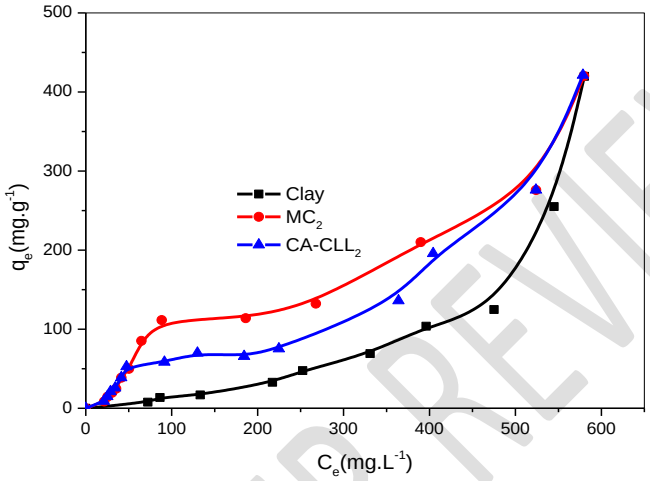

Fig. 9. Isotherms' adsorption of red Congo on adsorbent materials

3.4. Modelling of Congo red adsorption isotherms on three adsorbent materials

The mechanism of adsorption of Congo red by the materials was explained by the Langmuir, Freundlich and Tempkin models (Figs. 10, 11 and 12). The maximum adsorption capacities according to the Langmuir model are presented in Table 3. According to this model, activated carbon shows the highest amount of adsorbed Congo red molecules with 452 mg.g^{-1}. The Freundlich model ($R_F^2 > R_T^2 > R_L^2$)was found to be the most credible model to explain the adsorption of Congo red in liquid phase. In comparison the Freundlich model confirms the cooperative and multilayer adsorption of Congo red on the adsorbent materials.

- *Langmuir isotherm*

The isotherms were plotted according to the equation (12):

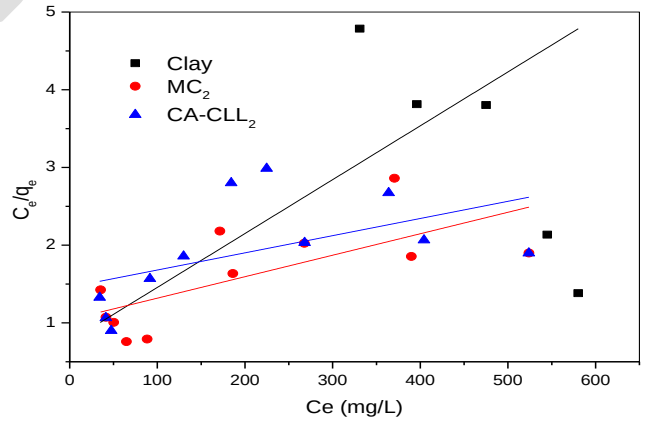

Fig. 10. Forms linearized of the model Langmuir for red Congo adsorption on the three adsorbent materials

♦ *Freundlichisotherm*

This model is presented according to the relation (14) :

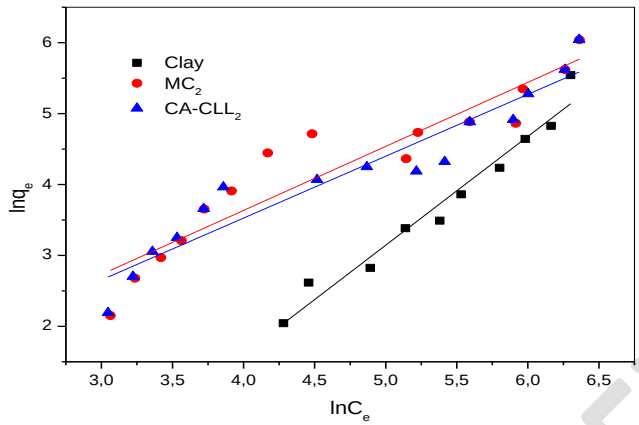

Fig. 11. Forms linearized of the model Freundlich for red Congo adsorption on the three adsorbent materials

♦ *Modèle de Tempkin*

This model was presented according to the equation (15):

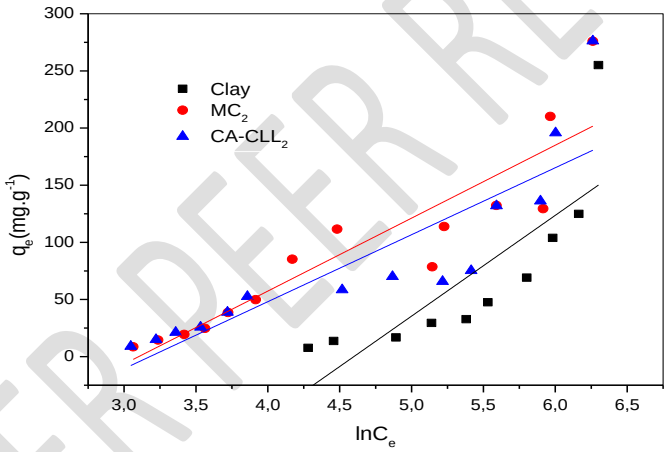

Fig. 12. Forms linearized of the model Tempkin for red Congo adsorption on the three adsorbent materials

Table 3. Parameter values of the Congo red adsorption isotherm models and comparison with other adsorbents.

	Langmuir isotherm			Freundlich isotherm			Tempkinisotherm			References
	q_{max}	K_L	R_L^2	1/n	K_F	R_F^2	A	B	R_T^2	
Clay	145.0	0.011	0.050	1.53	0.01	0.960	0.01	88.19	0.614	This work
MC_2	362.0	0.003	0.446	0.90	1.02	0.878	0.05	63.82	0.813	This work
$CA\text{-}CLL_2$	452	0.002	0.197	1.04	0.87	0.907	0.04	58.60	0.735	This work
CoMgAl-BLDO	990.1									[18]

Cellulose-GNP beads	139.6	[19]

3.5. Adsorption mechanism of red Congo on adsorbent materials[15]

During the adsorption of Congo red, several types of interaction can be noted. There are electrostatic interaction, hydrophobic interaction, hydrogen bonding interaction, π-π dispersion interaction and n-π interaction [20].

Fig. 13. Adsorption mechanism of red Congo on adsorbent materials[15].

We note that oxygenated functional groups, such as the carboxyl, carbonyl and hydroxyl groups of adsorbent materials, and the amino groups (-NH_2) of the Congo red molecule could be involved in the formation of hydrogen and carbon-nitrogen (C-N) bonds. This bonding could be promoted at high temperatures to form amide bonds. π - π dispersion interactions could take place between the π bonds of the adsorbent materials and the aromatic rings of the Congo Red molecules. In the presence of the adsorbent materials, we can observe that the sulphonate group (of the Congo Red molecules would be repelled by the negative sites of the substrate and the hydrophobic parts of the molecule can be trapped.

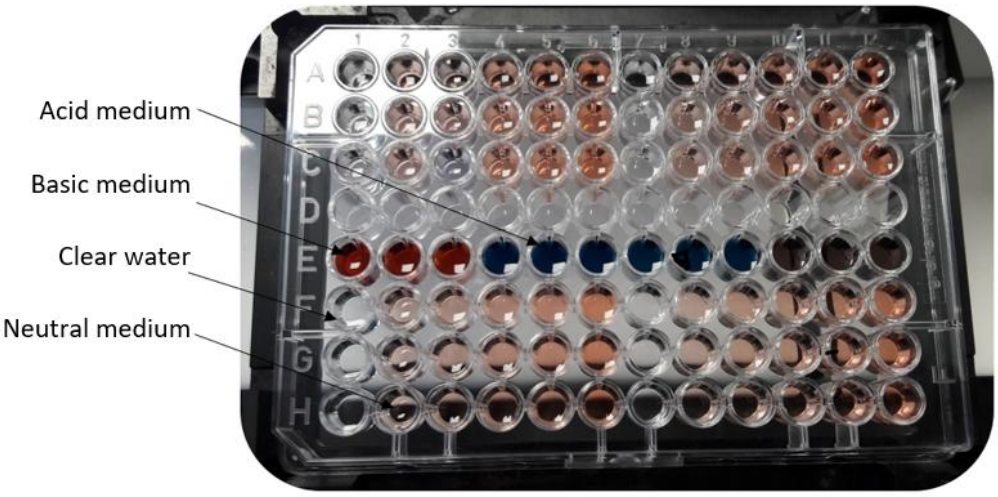

(a) Colours of Congo red during adsorption tests.

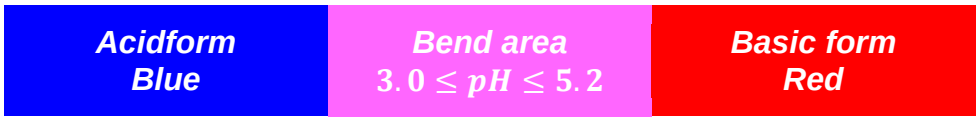

(b) Different colors of Congo red in aqueous media

Fig. 14. Behaviour of the Congo Red solution during adsorption tests in an aqueous medium.

Fig.14.(a) shows the behaviour of the Congo Red solution during the adsorption tests. The choice of carrying out the adsorption tests at the free pH of the pollutant solution showed the different changes in colour of Congo red as a coloured indicator. Its blue, pink and red colours in acid, neutral and basic media respectively were revealed during the test (Fig.14.b). When the Congo red is almost eliminated, the solution is almost clear. Subsequently, however, it reveals the nature of the polluting solution. It turns blue when the acidity provided by the adsorbent materials predominates, which can also be explained by the reduction of Congo red in the reaction medium. In addition, since a coloured indicator is an acid/base couple, the acid form could contribute to the increase in acidity. The pink colour indicates neutrality or pseudo-equivalence between the acidity and basicity of the Congo Red solution in the effluent. The red colouring shows the predominance of Congo red in solution, i.e. its basic form, so the carbonaceous material introduced was not sufficient to eliminate its molecules, even if it meant considerably reducing their level. This phenomenon could be avoided by adding a buffer, if we ensured that the Congo red molecules were selectively adsorbed to the detriment of the buffer molecules.

4. CONCLUSION

In this work, the chemical route was used to synthesize two adsorbent materials for comparison with natural clay for the adsorptive removal of Congo red. The kinetic study revealed that the adsorption process reached equilibrium before 60 min of reaction and obeyed the pseudo-second-order kinetics, thus the adsorption was chemical. The adsorption capacity determined by the Langmuir model is classified as follows CA - CLL_2> MC_2>Clay. The adsorption isotherm data correlate better with the Freundlich model. The composite material shows high dye removal efficiency and is more favourable to the adsorption of Congo red with$1/n < 1$. Nevertheless, all three adsorbent materials can be used for the removal of anionic dyes from industrial wastewater to comply with discharge standards.

Highlights

- Removal of anionic dye from aqueous solutions by varieties adsorbents: Kinetic and equilibrium studies.
- A variety of models are applied to fit isotherms and adsorption kinetics.
- Adsorption of red Congo on low-cost adsorbents.

RÉFÉRENCES

1. Lian Q, Islam F, Uddin Z, Lei X, Depan D. Chemosphere Enhanced adsorption of resorcinol onto phosphate functionalized graphene oxide synthesized via Arbuzov Reaction : A proposed mechanism of hydrogen bonding and π - π interactions. Chemosphere [Internet]. 2021;280:130730. Available from: https://doi.org/10.1016/j.chemosphere.2021.130730
2. Zhang X, Dianchen D, Sun P, Lian Q, Yao H. Chemosphere Goethite dispersed corn straw-derived biochar for phosphate recovery from synthetic urine and its potential as a slow-release fertilizer. Chemosphere [Internet]. 2021;262:127861. Available from: https://doi.org/10.1016/j.chemosphere.2020.127861
3. Kannan N, Sundaram MM. Kinetics and mechanism of removal of methylene blue by adsorption on various carbons — a comparative study. 2001;51:25–40.
4. Birol I, Volkan U. International Journal of Biological Macromolecules Adsorption of methylene blue on sodium alginate – flax seed ash beads : Isotherm , kinetic and thermodynamic studies. 2021;167:1156–67.
5. Allafchian A, Mousavi ZS, Hosseini SS. International Journal of Biological Macromolecules Application of cress seed musilage magnetic nanocomposites for removal of methylene blue dye from water. Int J BiolMacromol [Internet]. 2019;136:199–208. Available from: https://doi.org/10.1016/j.ijbiomac.2019.06.083

6. Singh S, Sidhu GK, Singh H. Removal of methylene blue dye using activated carbon prepared from biowaste precursor. Indian Chem Eng [Internet]. 2019;61:28–39. Available from: https://doi.org/10.1080/00194506.2017.1408431
7. Dehmani Y, El O, Mezougane H. Comparative study on adsorption of cationic dyes and phenol by natural clays. Chem Data Collect [Internet]. 2021;33:100674. Available from: https://doi.org/10.1016/j.cdc.2021.100674
8. Zhang Z, Moghaddam L, O'Hara IM, Doherty WOS. Congo Red adsorption by ball-milled sugarcane bagasse. Chem Eng J [Internet]. 2011;178:122–8. Available from: http://dx.doi.org/10.1016/j.cej.2011.10.024
9. Hameed BH, Din ATM, Ahmad AL. Adsorption of methylene blue onto bamboo-based activated carbon: Kinetics and equilibrium studies. J Hazard Mater. 2007;141:819–25.
10. Kilic M, Apaydin-Varol E, Pütün AE. Adsorptive removal of phenol from aqueous solutions on activated carbon prepared from tobacco residues: Equilibrium, kinetics and thermodynamics. J Hazard Mater. 2011;189:397–403.
11. Rao R, Huang Y, Ling Q, Hu C, Dong X, Xiang J, et al. A facile pyrolysis synthesis of Ni doped Ce2O3@CeO2/CN composites for adsorption removal of Congo red: Activation of carbon nitride structure. Sep PurifTechnol [Internet]. 2023;305:122505. Available from: https://doi.org/10.1016/j.seppur.2022.122505
12. Liu J, Wang N, Zhang H, Baeyens J. Adsorption of Congo red dye on FexCo3-xO4 nanoparticles. J Environ Manage. 2019;238:473–83.
13. Sogbochi E, Balogoun CK, Pascal C, Dossa A, Codjo D, Sohounhloue K. Evaluation of Adsorption Capacity of Methylene Blue in Aqueous Medium by Two Adsorbents : The Raw Hull of Lophira Lanceolata and Its Activated Carbon. 2017;6:76–87.
14. Sogbochi E, Nonviho G, Girods P, Fontana S. Removal of hydroxybenzene for the purpose of treating wastewater from the plastics industry using activated carbon obtained from Lophira lanceolata hulls . J Chem ,BiolPhys Sci. 2023;13.
15. Sogbochi E, Girods P, Nonviho G, Fontana S, Rogaume Y, Codjo D, et al. Use of Carbonaceous Materials Derived from Co-products of Lophira lanceolata for Adsorption Tests of Congo Red Dye. Am J Phys Chem. 2022;11:91–101.
16. Foo KY, Hameed BH. Insights into the modeling of adsorption isotherm systems. Chem Eng J. 2010;156:2–10.
17. Lütke SF, Igansi A V, Pegoraro L, Dotto GL, Pinto LAA, Cadaval TRS. Journal of Environmental Chemical Engineering Preparation of activated carbon from black wattle bark waste and its application for phenol adsorption. J Environ Chem Eng [Internet]. 2019;7:103396. Available from: https://doi.org/10.1016/j.jece.2019.103396
18. Miao J, Zhao X, Zhang Y, Lei Z, Liu Z. Applied Clay Science Preparation of hollow hierarchical porous CoMgAl-borate LDH ball-flower and its calcinated product with extraordinary adsorption capacity for Congo red and methyl orange. Appl Clay Sci [Internet]. 2021;207:106093. Available from: https://doi.org/10.1016/j.clay.2021.106093
19. González-López ME, Laureano-Anzaldo CM, Pérez-Fonseca AA, Gómez C, Robledo-Ortíz JR. Congo red adsorption with cellulose-graphene nanoplatelets beads by differential column batch reactor. J Environ Chem Eng. 2021;9.
20. Pauletto PS, Lütke SF, Dotto GL, Salau NPG. Adsorption mechanisms of single and simultaneous removal of pharmaceutical compounds onto activated carbon: Isotherm and thermodynamic modeling. J Mol Liq [Internet]. 2021;336:116203. Availablefrom: https://doi.org/10.1016/j.molliq.2021.116203